



Characterization of Ceramic Membrane based on Calcium Carbonate from Onyx Stone and Its Application for Coconut Sap Treatment

H. Aripin^{1*}, E. Priatna, D. Dedi², I. N. Sudiana³, S. Sabchevski⁴

¹Department of Electrical Engineering, Faculty of Engineering, Siliwangi University, Tasikmalaya, West Java, Indonesia.

²Research Centre for Electronics and Telecommunication, Indonesian Institute of Sciences, Bandung 40135, Indonesia

³Department of Physics, Faculty of Mathematics and Natural Sciences, Haluoleo University, Kendari Indonesia.

⁴Lab. Plasma Physics and Engineering, Institute of Electronics of the Bulgarian Academy of Sciences, Sofia, Bulgaria.

PAPER INFO

Paper history:

Received 16 September 2021

Received in revised form 28 October 2021

Accepted 04 29 October 2021

Keywords:

ceramic membrane, calcium carbonate, onyx stone, zeolite, silica xerogel, coconut sap, sap permeate flux

A B S T R A C T

In this study, the calcium carbonate from onyx stone used as a pore-forming agent in the ceramic membrane of kaolin, zeolite, and silica xerogel composites were investigated. Four different membrane samples were prepared with varying onyx stone content from 5 wt.% to 30 wt.% into composite and then the prepared samples were sintered at 1200°C. The structural properties of the prepared sample was investigated in detail using X-ray diffraction (XRD), Fourier transform infrared (FTIR) spectroscopy, Scanning Electron Microscopy (SEM), and N₂ adsorption-desorption isotherms. The removal performance of the membrane was successfully tested during coconut sap treatment. It has been found that the prepared samples have a porous structure made up of interconnected pores and their volume fraction depends on onyx stone content. The sample with the onyx stone content of 30 wt.% provides the largest volume fraction of homogeneously interconnected pores and its presence demonstrates the largest value for sap permeate flux and the flux rate in the initial phase. The pores formed in this produced membrane provide favorable conditions for the removal of the non-sugar impurities in the coconut sap.

doi: 10.5829/ije.2022.35.02b.05

1. INTRODUCTION

The coconut sap is the raw material derived from the coconut tree for production of sugar. In addition to sucrose, it also contains about 50% of non-sugar impurities such as soluble and insoluble organic and inorganic materials, amino acid, etc., which come from coconut plant cultivation place and raw sap production process [1]. Because the sap is converted into coconut sugar through a heating process, then during heating the sap undergoes chemical and physical changes such as caramelization of sugar. As a result, the impurities deteriorate the product quality of the produced sugar and dietary nutritional as the dark brown color, hard texture, reducing protein contents, and degradation of amino acid. Therefore, they must be removed before the thermal treatment of sap. Such consideration inspires us

to look for a way out to remove the non-sugar impurities from the coconut sap. As one of the most promising technologies, the ceramic membranes have been selected as an alternative approach for the treatment of coconut sap.

Many studies on membrane separation technology (MST) have been carried out for sugar processing. The MST utilization has been reported for use in an ultrafiltration membrane (UF) and it inflicts positive changes in the quality of sugar (e.g. increased purity, reduced turbidity, natural color, higher Brix value (°Bx), and protein content) [2]. When the UF is replaced by a reverse osmosis (RO) membrane for clarification of sugarcane juice an increase in the Brix value of the syrup concentrate has been observed as well [2]. The fact that both UF and RO polymer membranes are not resistant to organic solvents is a serious drawback. To overcome this, ceramic membranes have been developed. Microfiltration (MF) membrane formed as

*Corresponding Author Institutional Email: aripin@unsil.ac.id (H. Aripin)

ceramic pipes have been prepared from $\text{TiO}_2/\alpha\text{-Al}_2\text{O}_3$ and used to purify sugar cane juice [3]. MF membrane pores with a diameter of $0.6\ \mu\text{m}$ is effective in reducing turbidity and improving the color of sugarcane juice by about 92% and 16%, respectively. Furthermore, two tubular membranes of $\text{TiO}_2/\alpha\text{-Al}_2\text{O}_3$ composites (pore sizes of $0.1\ \mu\text{m}$ and $0.3\ \mu\text{m}$) have been investigated for their use in clarifying the sugarcane juice [4]. The purification process has produced a good result with the degree of turbidity and color removal as much as 99.4% and 44.8%, respectively. When the pore diameter of the UF membrane is reduced to $0.5\ \mu\text{m}$ [5], the turbidity and color of sugarcane juice reduce to 89.96% and 10.42%, respectively. The results of these studies have shown that the membranes of TiO_2 and Al_2O_3 composites have several advantages such as good resistance to thermal and organic solvents, and a longer lifetime compared with the polymer membranes. However, the raw materials prepared are expensive and their economic feasibility is less useful. Another drawback is that the formation of such ceramics requires very high temperatures of about 1600°C [6]. Several attempts have been made to reduce production costs and to lower the firing temperature of the ceramic membrane. For example, adding clay to Al_2O_3 has allowed a significant reduction in pore size of multichannel ceramic membrane [7]. It was reported that the pore size of clay and Al_2O_3 composite ceramic sintered at 1100°C were about $1\ \mu\text{m}$. In another study, the ceramic membrane prepared from corn cob ash at 1100°C has demonstrated a flexural strength value of 31 MPa and a pore size value of $0.13\ \mu\text{m}$ [8]. These studies have revealed that the properties of ceramic membranes depend strongly on porosity. Therefore, by controlling porosity, it is possible to obtain an appropriate performance of the membrane.

Recently, SiO_2 (silica xerogel) ceramic has been prepared using a sago waste ash [9] and geothermal sludge [10] as a starting powder. Amorphous silica xerogels have micro-to nanopore sizes and they have poor mechanical properties (e.g. fragility) which do not allow to form a single mechanical unit in water. Furthermore, in the reports on zeolite ceramic membranes, the pore size formed in the range of $0.1\ \mu\text{m}$ to $0.4\ \mu\text{m}$, the membrane has a great potential to remove impurities from coconut sap [11] and waste water [12]. However the membranes are limited in their mechanical strengths, so it causes a rapid membrane breakage when the applied pressure is in the range of 1 to 5 bars in the operation. One way to produce a ceramic membrane of the xerogel silica and zeolite composite with high mechanical strength and porosity is to add a pore-forming and plasticity agents in the composite.

Calcium carbonate (CaCO_3) can be added as a pore-forming agent and kaolin as a plasticity agent in the composition of the xerogel silica and zeolite composite

for porous ceramic membranes. CaCO_3 decomposes into calcium oxide (CaO) and carbon dioxide (CO_2) at a temperature of above 650°C . The empty spaces formed by the release of CO_2 gas bubbles during the sintering impart a porous texture to the membrane [13]. Because the commercially available CaCO_3 is expensive, it is replaced by CaCO_3 from onyx stone. It is reported that the main phase of the onyx stone composed of CaCO_3 in the form of the calcite mineral [14]. The purpose of this work is to produce low-cost ceramic membrane made from silica xerogel and abundant inexpensive inorganic materials like zeolite, kaolin, and onyx stone. In this paper, we discuss the influence of different onyx stone content on the structural properties of the membranes and evaluate their performance for coconut sap treatment.

2. MATERIAL AND METHODS

2.1. Materials and Membrane Sample Preparation

The raw materials for the prepared membranes are silica xerogel, zeolite, onyx stone and kaolin. The silica xerogel was prepared from sago waste ash by extract method. The extraction steps have been described in detail in previous studies [9]. The other raw materials were prepared from natural materials in Karangnunggal, Tasikmalaya, Indonesia. After cleaning and drying, they were ground using milling machine to pass through a $100\ \mu\text{m}$ sieve.

Table 1 presents the compositional formulations for the prepared membrane samples. For example, the M1 sample was prepared using the composition on a dry basis of 60 wt.% silica xerogel, 30 wt.% zeolite, 5 wt.% onyx stone, and 5 wt.% kaolin. Then, it was mixed with 4 mL polyvinyl alcohol (2 wt.%) solution and then stirred at 50°C for two hours. The mixture has been heated at 50°C until all solvent was evaporated. The resultant mixture is inserted into a circular disk-type mold with a size of 55 mm in diameter and 5 mm in thickness. The molded sample was dried in an oven at 100°C for 24 hours. The M2, M3, and M4 samples were prepared following the same steps.

2.2. Sintering the prepared membrane sample

The prepared membrane samples were sintered at a heating rate of $5^\circ\text{C}/\text{min}$ up to the temperature of 1200°C in the air using an electric furnace. The constant temperature at 1200°C for 2 hours is treated on the sample during sintering. The cooling was performed by natural convection after turning off the electric furnace and leaving the samples inside. The samples of M1, M2, M3, and M4 sintered at 1200°C are labeled by CM1, CM2, CM3, and CM4, respectively.

TABLE 1. The compositional formulations for the prepared membrane sample

Sample	Mass percentages (wt.%)			
	Silica xerogel	Zeolite	Onyx stone	Kaolin
M1	60	30	5	5
M2	60	20	15	5
M3	60	15	20	5
M4	60	5	30	5

2.3. Characterization

In this study, the contents of various oxides for the raw material was determined by the XRF measurements using an instrument of the Philips PW2400 wavelength-dispersive spectrometer. During measurement, the instrument operates at a voltage of 24 kV, a current of 100 mA, and collimator mask of 27 mm, and it uses the Rh-X ray tube as an excitation source. Furthermore, the crystalline phases of the sample were identified by a Smartlab X-ray diffractometer with having Cu K α radiation at 0.15418 nm. The operating voltage and the current used were 40 kV and 30 mA, respectively. The sample functional groups of were tested by a Varian 800 Fourier FTIR spectrometer. The data recorded is in the wavelength range from 400 to 4000 cm⁻¹ and the spectral resolution is 4 cm⁻¹. The KBr pellet technique was used for reflecting the FTIR spectra at room temperature. The fracture surfaces of the samples were imaged by SEM at a magnification of 5000 times and an operating voltage of 5 kV. The pore properties of sample were tested by a nitrogen adsorption-desorption method (Quantachrome, Nova-1000).

2.4. Permeation Experiments

The detailed experimental procedures for coconut sap permeation are described elsewhere [11]. The concentration of coconut sap used for the experiment was 0.86 g/L. The permeation parameters were calculated using the equation for permeate flux [15].

TABLE 2. Contents of various oxides for the raw material

Oxide constituent	Silica xerogel (wt.%)	Zeolite (wt.%)	Onyx stone (wt.%)	Kaolin (wt.%)
SiO ₂	98.81	59.30	0.20	42.20
TiO ₂	0.01	0.70	ND	1.10
ZrO ₂	ND	5.02	1.80	0.46
MgO	ND	0.12	1.09	ND
Al ₂ O ₃	0.41	5.02	0.08	24.80
Na ₂ O	0.12	ND	ND	30.10
Fe ₂ O ₃	0.11	8.47	14.7	1.11
K ₂ O	0.34	12.30	0.12	ND
CaO	0.14	7.81	82.0	ND
LOI	0.04	1.27	0.01	0.23

3. RESULTS AND DISCUSSIONS

Table 2 presents the contents of various oxides for silica xerogel, zeolite, onyx stone, and kaolin. The SiO₂ is the main oxide constituent for silica xerogel, zeolite and kaolin, whereas the CaO is for onyx stone. The ZrO₂, Al₂O₃, Fe₂O₃, K₂O, and CaO contribute to significant amount of oxide content for zeolite. The presence of loss on ignition (LOI) in all raw material is related to additional components of volatile, organic mater and hydroxides.

Figure 1a presents the XRD patterns of the unsintered membrane sample and those sintered at 1200°C. It reveals that the crystalline phases detected for the unsintered sample (M1) consists of kaolin at $2\theta = 20.9^\circ$ and 24.9° [16-18], quartz, zeolite at $2\theta = 27.2^\circ$ [19], and calcite (CaCO₃) at $2\theta = 30^\circ$. In the sample sintered at 1200°C (CM1), a zeolite crystal is formed followed by cristobalite, mullite (3Al₂O₃2SiO₂), and then by the crystallization of gehlenite (Ca₂Al₂SiO₇). and anorthite (Ca₂Al₂Si₂O₈). It can be observed that the calcite phase disappears in the sintered sample and it is replaced by an gehlenite and anorthite phases. It was thought that gehlenite phase is as a reaction result between the metakaoline and calcium. Anorthite is formed from silica, aluminum oxide and gehlenite. Such interpretation agrees with the observed results of the XRD pattern for samples prepared from a mixture of metakaoline and calcium oxide based stone [20]. As the content of onyx stone increases, the intensity peak of anorthite increase, whereas that of crystalline cristobalite and mullite decreases. It indicates that the anorthite is an unstable intermediate phase.

Figure 1b presents the FTIR spectra of the sample sintered at 1200°C. The absorption band of peak 1 at about 464 cm⁻¹ is associated to tetrahedral Si–O bending vibrations, which is characteristic of the starting metakaoline [17]. The intensity decreases as the onyx stone content increases. In the case of higher onyx stone content, most of the metakaoline particles can react with calcite. The absorption band of peak 2 and 4 at about 538 cm⁻¹ and 775 cm⁻¹ is related to anorthite characteristics (Si–O–Al bond) [21]. The peaks at 626 cm⁻¹ (3) that is ascribed to crystalline cristobalite [18]. The peak 5 near 800 cm⁻¹ and the strong absorption band of the peak 6 at 1100 cm⁻¹ are related to the Si–O–Si bonds for the symmetric and anti-symmetric stretching vibrations, respectively [22]. The absorption band of peaks 7 located at about 3420 cm⁻¹ is assigned to the H–O–H bonds. The bands is the characteristic for the adsorbed water molecules. Respectively, the peaks 8, 9, and 10 that appear at 3600, 3680, 3800 cm⁻¹ correspond to the kaolinite [18].

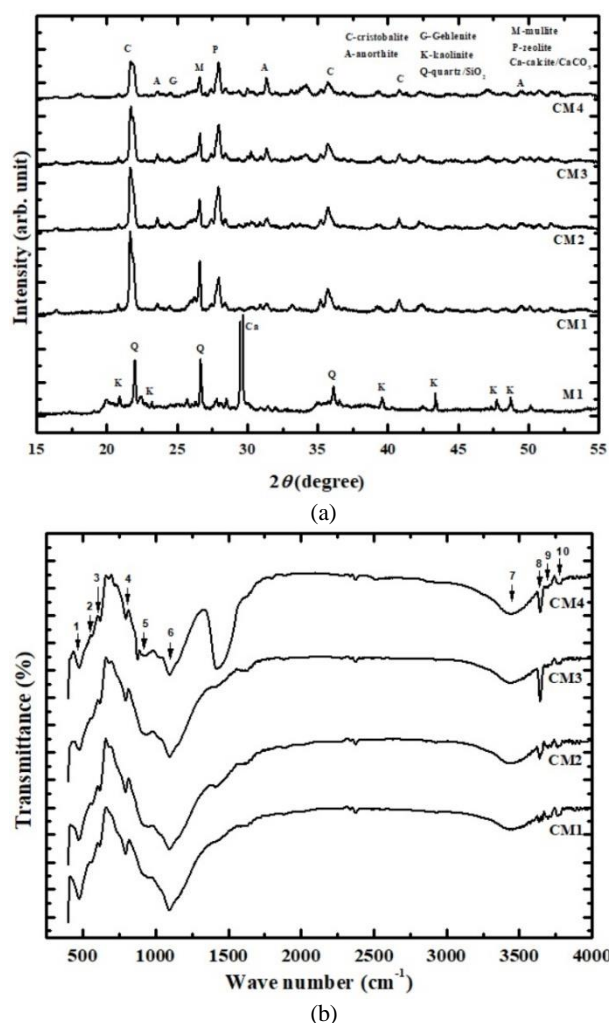


Figure 1. XRD patterns and (b) FTIR spectra of the unsintered membrane (M1) and membranes sintered at 1200°C (CM)

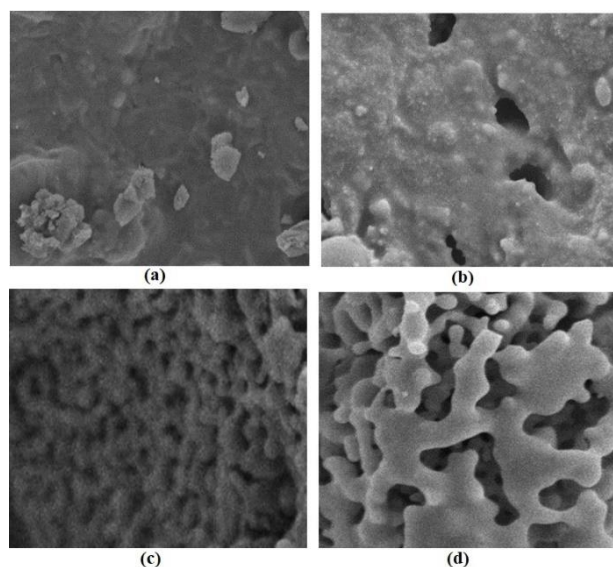


Figure 2. SEM images of (a) CM1, (b) CM2, (c) CM3, and

(d) CM4

Figure 2 presents the SEM images of the CM samples at different content of the onyx stone. For CM1, the microstructure is characterized by rough surface texture with small and inhomogeneous pores. Their pores are not evenly distributed. In the CM2 sample, in some locations, a few larger isolated pores and open pores are present. Furthermore, the opened and interconnected array of pores are characteristic for the sample CM3. The texture of the CM4 sample is similar to that of the CM3 sample, although the CM3 presents a much denser structure with more uniform pores. As a whole, the analysis of the SEM images indicates that the addition of onyx stone with content larger than 20% results in homogeneous, interconnected, and organized pores with a highly porous structure. The pores are produced due to the escapement of the gases [13] and ceramic expansion by the formation of crystalline anorthite and gehlenite during sintering [23]. From this SEM observation, it can be said that the samples with an onyx stone content of 10 wt.% (CM1) and 20 wt.% (CM2) shows isolated pores and poor porosity if compared with other samples. This is due to the limited connections of the small pores in the MC1 and MC2 samples. In all other (MC3 and MC4) the addition of onyx stone changes the appearance of the ceramic surface which becomes more porous.

Figures 3a and 3b show the N₂ gas adsorption-desorption isotherms at 77 K and pore size distributions of CM sample sintered at 1200°C, respectively. According to the recognized classification of International Union of Pure and Applied Chemistry (IUPAC), the shape of N₂ gas adsorption-desorption isotherm and hysteresis loop of the sintered membrane samples are type IV and type H3, respectively [24], which is characteristic of a slit-type mesoporous structure. In the isotherm, the adsorption increases slowly as the relative pressure increases up to about P/P₀= 0.9 and after that rapid adsorption can be observed in the samples. As shown in Figure 3a, the N₂ uptake increases as the onyx stone content increases in the sample, which may be associated with a higher mesopore ratio. It can be understood that at 1200°C, the higher content of onyx stone in the sample results in more vacant spaces created by the release of CO₂ gas bubbles. This is in line with the interpretation of the results for the CaO/SiO₂ composite, where the porosity tends to increase with increasing the ratio up to 38% [25]. According to pore size distribution in Figure 3b, one could clearly see that the log differential intrusion increases with increasing the onyx stone content. This increase is attributed to an increase in the volume fraction of the interconnected pores [26], which inevitably results in an increased total porosity in the

ceramic membrane. Thus, the CM4 sample has the largest fraction of interconnected pores.

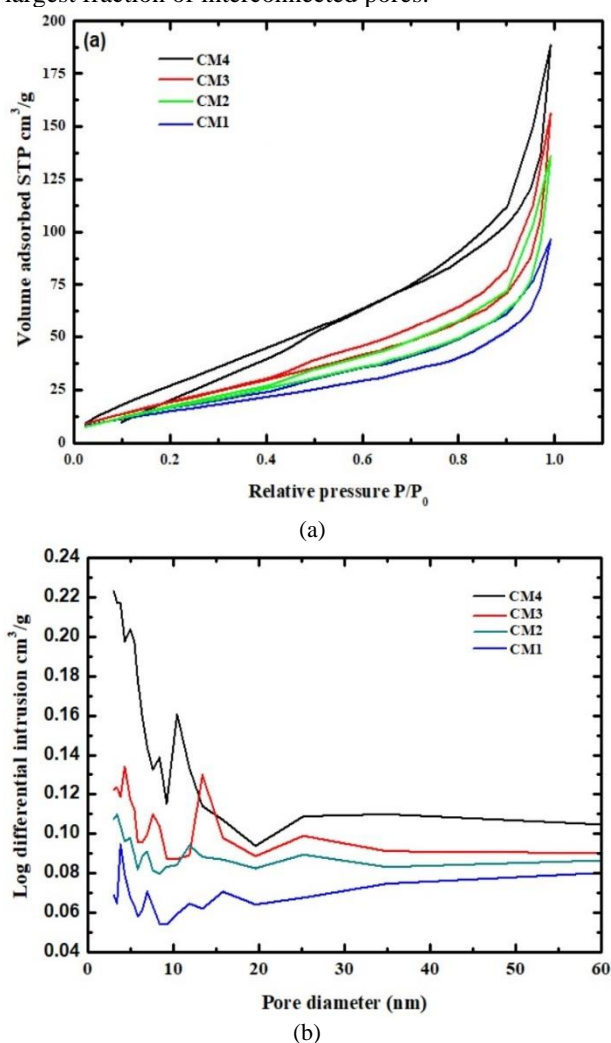


Figure 3. (a) Typical N₂ adsorption-desorption isotherms, and (b) pore size distributions of the sintered membrane sample

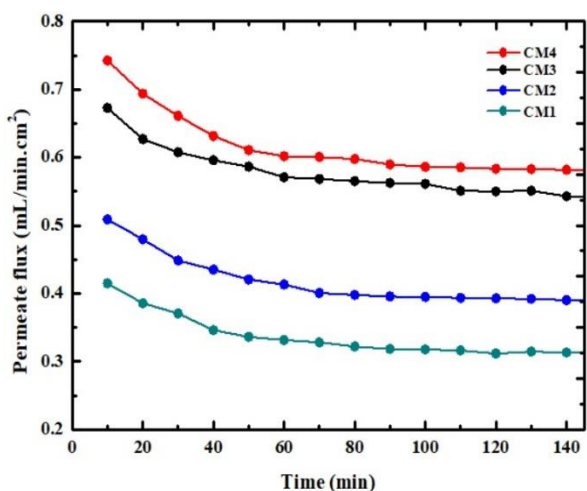


Figure 4. Change of the sap permeate flux with time for ceramic membranes with a different onyx stone content

Figure 4 presents the change of the sap permeate flux with respect to time for ceramic membranes with a different onyx stone content. The sap permeate flux values increased with an increasing onyx stone content. The initial permeate fluxes gradually increase from 0.44 to 0.68 mL/min.cm² for the onyx stone content in the interval from 5 wt.% (CM1) to 30 wt.% (CM4), respectively. As can be seen in Figures 4 and 3b, obviously, there is a clear correlation between the flux and the log differential intrusion. Therefore, this flux increase is due to an increase in the volume fraction of the interconnected pores. CM3 and CM4 samples have greater fluxes than CM1 and CM2. In this case, CM3 and CM4 have a greater volume fraction of interconnected pores than CM1 and CM2, so that its presence accelerates the process of separating impurities from coconut sap through the pores. Its largest flux value is higher than that obtained for ceramic membrane prepared from the sintered zeolite [11]. Furthermore, the values of the sap permeate flux also decrease gradually with time, and initially, their value decreases at different rates until the same time of about 80 min and finally reach a constant value. The decrease in flux value is due to a reduction in the volume fraction of interconnected pores. In the case, the pores are blocked by a deposited layer of impurities from non-sugar ingredients during operation [27]. As time increases, more and more impurities fill the volume of the interconnected pores. This behavior was also found in the studies on water purification [28] using ceramic membranes. Furthermore, in the initial phase, the flux rate increases as the onyx stone content increases. It is attributed to the presence of the larger volume fraction of large mesopores (pore size greater than 20 nm). The volume fraction of large pores gradually increases with increasing onyx content. Thus, smaller impurity particles tend to be rejected by the membrane having smaller pores and are more likely to enter larger pores and create more polarized impurity layers. This is consistent with the previous findings reported by Novoa et al. [29], where the formation of a deposited layer occurs in larger pores.

4. CONCLUSION

A porous ceramic membrane for the treatment of coconut sap has been successfully produced from a sintered composition made of kaolin, zeolite, onyx stone, and silica xerogel. In it, the onyx stone is used as a pore-forming agent. The prepared ceramic membrane have a porous structure made up of interconnected pores with a relatively high volume fraction of pores that depends on onyx stone content. The pores were developed due to release of CO₂ and ceramic expansion by the formation of crystalline anorthite and gehlenite.

The membran sample with an onyx stone content of 30 wt.% has demonstrated the largest value of the sap permeate flux and the flux rate in the initial phase. As a whole, the experimental results demonstrate that the calcium carbonate from onyx stone is an appropriate pore-forming agent for ceramic membrane. The obtained data can be used for an envisaged further optimization of the properties of this promising material.

5. ACKNOWLEDGMENTS

This research was funded by Minister of Education, Cultural, Research and Technology, Republic of Indonesia through the Project of Higher Education Applied Research in 2018 (Contract Number: 091/SP2H/LT/DRPM/2018).

6. REFERENCES

- Pandiselvam, R., Manikantan, M., Binu, S.M., Ramesh, S., Beegum, S., Gopal, M., Hebbar, K., Mathew, A., Kothakota, A. and Kaavya, R., "Reaction kinetics of physico-chemical attributes in coconut inflorescence sap during fermentation", *Journal of Food Science and Technology*, Vol. 58, No., (2021), 1-9. DOI: 10.1007/s13197-021-05088-3.
- Jegatheesan, V., Shu, L., Phong, D.D., Navaratna, D. and Neilly, A., "Clarification and concentration of sugar cane juice through ultra, nano and reverse osmosis membranes", *Membrane Water Treatment*, Vol. 3, No. 2, (2012), 99-111. DOI: 10.12989/mwt.2012.3.2.099.
- Moreno, R.M.C., de Oliveira, R.C. and de Barros, S.T.D., "Comparison between microfiltration and addition of coagulating agents in the clarification of sugar cane juice", *Acta Scientiarum. Technology*, Vol. 34, No. 4, (2012), 413-419. DOI: 10.4025/actascitechnol.v34i4.8890.
- dos Santos Gaschi, P., dos Santos Gaschi, P., Barros, S.T.D. and Pereira, N.C., "Pretreatment with ceramic membrane microfiltration in the clarification process of sugarcane juice by ultrafiltration", *Acta Scientiarum. Technology*, Vol. 36, No. 2, (2014), 303-306. DOI: 10.4025/actascitechnol.v36i2.17322.
- Li, W., Ling, G., Lei, F., Li, N., Peng, W., Li, K., Lu, H., Hang, F. and Zhang, Y., "Ceramic membrane fouling and cleaning during ultrafiltration of limed sugarcane juice", *Separation and Purification Technology*, Vol. 190, No., (2018), 9-24. DOI: 10.1016/j.seppur.2017.08.046.
- Landek, D., Ćurković, L., Gabelica, I., Kerolli Mustafa, M. and Žmak, I., "Optimization of sintering process of alumina ceramics using response surface methodology", *Sustainability*, Vol. 13, No. 12, (2021), 6739. DOI: 10.3390/su13126739.
- Souza, M.Y.M.d., Lira, H.d.L., Santana, L.N.d.L. and Rodríguez, M.A., "Preparation and application in crude oil-water separation of clay-based membranes", *Materials Research*, Vol. 24, No., (2021). DOI: 10.1590/1980-5373-MR-2020-0508.
- Kamarudin, N., Harun, Z., Othman, M.D., Hubadillah, S., Jamaluddin, M. and Yusof, K., "Preliminary characterization of corn cob ash as an alternative material for ceramic hollow fiber membrane (chfm/cca)", *International Journal of Engineering, Transactions B: Applications*, Vol. 31, No. 8, (2018), 1389-1397. DOI: 10.5829/ije.2018.31.08b.30.
- Aripin, H., Mitsudo, S., Sudiana, I.N., Tani, S., Sako, K., Fujii, Y., Saito, T., Idehara, T. and Sabchevski, S., "Rapid sintering of silica xerogel ceramic derived from sago waste ash using sub-millimeter wave heating with a 300 ghz cw gyrotron", *Journal of Infrared, Millimeter, and Terahertz Waves*, Vol. 32, No. 6, (2011), 867-876. DOI: 10.1007/s10762-011-9797-2.
- Widiyandari, H., Pardoyo, P., Sartika, J., Putra, O., Purwanto, A. and Ernawati, L., "Synthesis of mesoporous silica xerogel from geothermal sludge using sulfuric acid as gelation agent", *International Journal of Engineering, Transactions A: Basics*, Vol. 34, No. 7, (2021), 1569-1575. DOI: 10.5829/ije.2021.34.07a.02.
- Aripin, H., Busaeri, N., Gufroni, A.I. and Sabchevski, S., "Activated natural zeolite membrane for separating dissolved impurities in coconut sap", in *Materials Science Forum*, Vol. 1000, No. Issue, (2020), 293-302. DOI: 10.4028/www.scientific.net/MSF.1000.293.
- Othman, M.D., Adam, M., Hubadillah, S.K., Puteh, M.H., Harun, Z. and Ismail, A., "Evaluating the sintering temperature control towards the adsorptivity of ammonia onto the natural zeolite based hollow fibre ceramic membrane", *International Journal of Engineering, Transactions B: Applications*, Vol. 31, No. 8, (2018), 1398-1405. DOI: 10.5829/ije.2018.31.08b.31.
- Gilstrap, W.D., Meanwell, J.L., Paris, E.H., López Bravo, R. and Day, P.M., "Post-depositional alteration of calcium carbonate phases in archaeological ceramics: Depletion and redistribution effects", *Minerals*, Vol. 11, No. 7, (2021), 749. DOI: <https://doi.org/10.3390/min11070749>.
- Quiroga-González, E. and Morales-Merino, E., "Mexican onyx waste as active material and active material's precursor for conversion anodes of lithium ion batteries", *Frontiers in Energy Research*, Vol. 9, No., (2021), 41. DOI: 10.3389/fenrg.2021.593574.
- Bagheripour, E., Moghadassi, A. and Hosseini, S.M., "Incorporated poly acrylic acid-co-fe3o4 nanoparticles mixed matrix polyethersulfone based nanofiltration membrane in desalination process", *International Journal of Engineering, Transactions C: Aspects*, Vol. 30, No. 6, (2017), 821-829. DOI: 10.5829/ije.2017.30.06c.01.
- Svergzova, S., Miroshnichenko, N., Shaikhiev, I., Sapronova, Z., Fomina, E., Shakurova, N. and Promakhov, V., "Application of sorbent waste material for porous ceramics production", *International Journal of Engineering, Transactions C: Aspects*, Vol. 34, No. 3, (2021), 621-628. DOI: 10.5829/ije.2021.34.03c.05.
- Yang, X., Yang, W. and Hu, J., "Preparation of low-dielectric-constant kaolin clay ceramics by chemical cleaning method", *Frontiers in Materials*, Vol. 8, No., (2021), 198. DOI: 10.3389/fmats.2021.692759.
- Valášková, M., Blahůšková, V. and Vlček, J., "Effects of kaolin additives in fly ash on sintering and properties of mullite ceramics", *Minerals*, Vol. 11, No. 8, (2021), 887. DOI: 10.3390/min11080887.
- Shi, J.Z., Zhu, X.L., Li, L. and Chen, X.M., "Zeolite ceramics with ordered microporous structure and high crystallinity prepared by cold sintering process", *Journal of the American Ceramic Society*, Vol. 104, No. 11, (2021), 5521-5528. DOI: 10.1111/jace.17964.
- Simão, L., Caldato, R., Innocentini, M. and Montedo, O., "Permeability of porous ceramic based on calcium carbonate as pore generating agent", *Ceramics International*, Vol. 41, No. 3, (2015), 4782-4788. DOI: 10.1016/j.ceramint.2014.12.031.
- Harabi, A., Zaiou, S., Guechi, A., Foughali, L., Harabi, E., Karboua, N.-E., Zouai, S., Mezahi, F.-Z. and Guerfa, F., "Mechanical properties of anorthite based ceramics prepared from kaolin dd2 and calcite", *Cerâmica*, Vol. 63, No., (2017), 311-317. DOI: 10.1590/0366-69132017633672020.

22. Popescu, C.-M. and Broda, M., "Interactions between different organosilicons and archaeological waterlogged wood evaluated by infrared spectroscopy", *Forests*, Vol. 12, No. 3, (2021), 268. DOI: <https://doi.org/10.3390/f12030268>.
23. Simão, L., Montedo, O.R.K., Caldato, R., Innocentini, M.D.d.M., da Silva Paula, M.M., Angioletto, E., Dal-Bó, A.G. and da Silva, L., "Porous ceramic structures obtained from calcium carbonate as pore generating agent", in *Materials Science Forum*, Vol. 775, No. Issue, (2014), 755-760. DOI: [10.4028/www.scientific.net/MSF.775-776.755](https://doi.org/10.4028/www.scientific.net/MSF.775-776.755).
24. Yang, W., Li, C., Tian, S., Liu, L. and Liao, Q., "Influence of synthesis variables of a sol-gel process on the properties of mesoporous alumina and their fluoride adsorption", *Materials Chemistry and Physics*, Vol. 242, No., (2020), 122499. DOI: [10.1016/j.matchemphys.2019.122499](https://doi.org/10.1016/j.matchemphys.2019.122499).
25. Yang, Z., Lin, Q., Lu, S., He, Y., Liao, G. and Ke, Y., "Effect of cao/sio2 ratio on the preparation and crystallization of glass-ceramics from copper slag", *Ceramics International*, Vol. 40, No. 5, (2014), 7297-7305. DOI: [10.1016/j.ceramint.2013.12.071](https://doi.org/10.1016/j.ceramint.2013.12.071).
26. Es-saddik, M., Laasri, S., Taha, M., Laghzizil, A., Guidara, A., Chaari, K., Bouaziz, J., Hajjaji, A. and Nunzi, J., "Effect of the surface chemistry on the stability and mechanical properties of the zirconia-hydroxyapatite bioceramic", *Surfaces and Interfaces*, Vol. 23, No., (2021), 100980. DOI: [10.1016/j.surfin.2021.100980](https://doi.org/10.1016/j.surfin.2021.100980).
27. Yang, M., Zhao, C., Zhang, S., Li, P. and Hou, D., "Preparation of graphene oxide modified poly (m-phenylene isophthalamide) nanofiltration membrane with improved water flux and antifouling property", *Applied Surface Science*, Vol. 394, No., (2017), 149-159. DOI: [10.1016/j.apsusc.2016.10.069](https://doi.org/10.1016/j.apsusc.2016.10.069).
28. Arumugham, T., Kaleekkal, N.J., Gopal, S., Nambikkattu, J., Rambabu, K., Aboulella, A.M., Wickramasinghe, S.R. and Banat, F., "Recent developments in porous ceramic membranes for wastewater treatment and desalination: A review", *Journal of Environmental Management*, Vol. 293, No., (2021), 112925. DOI: [10.1016/j.jenvman.2021.112925](https://doi.org/10.1016/j.jenvman.2021.112925).
29. Novoa, A.F., Vrouwenvelder, J.S. and Fortunato, L., "Membrane fouling in algal separation processes: A review of influencing factors and mechanisms", *Frontiers in Chemical Engineering*, Vol. 3, No., (2021), 21. DOI: [10.3389/fceng.2021.687422](https://doi.org/10.3389/fceng.2021.687422).

Persian Abstract

چکیده

در این مطالعه، کربنات کلسیم از سنگ اونیکیس به عنوان عامل منفذ ساز در غشای سرامیکی کامپوزیت های کانولن، زئولیت و سیلیس زیروژل مورد بررسی قرار گرفت. چهار نمونه غشایی مختلف با محتوای سنگ اونیکیس متفاوت از ۵ درصد وزنی تا ۳۰ درصد وزنی به کامپوزیت تهیه و سپس نمونه های آماده شده در دمای ۱۲۰۰ درجه سانتیگراد ت حرارت دیدند. خواص ساختاری نمونه تهیه شده با استفاده از پراش پرتو ایکس (XRD)، طیف سنجی فرسرخ تبدیل فوریه (FTIR)، میکروسکوپ الکترونی روبشی (SEM) و ایزوترم های جذب-واجذبی N2 مورد بررسی قرار گرفت. عملکرد حذف غشا با موفقیت در طول تسویه پساب شیر نارگیل آزمایش شد. مشخص شده است که نمونه های تهیه شده دارای ساختار متخلخل هستند که از منافذ به هم پیوسته تشکیل شده است و کسر حجمی آنها به محتوای سنگ اونیکیس بستگی دارد. نمونه با محتوای سنگ اونیکیس ۳۰ درصد وزنی، بزرگترین کسر حجمی از منافذ همگن به هم پیوسته را فراهم می کند و حضور آن بیشترین مقدار را برای شار نفوذ شیر و نرخ شار در فاز اولیه نشان می دهد. منافذ تشکیل شده در این غشای ساخته شده شرایط مطلوبی را برای حذف ناخالصی های غیر قندی موجود در شیر نارگیل فراهم می کند.
